

# Geophysical expression of the Raudfjellet ophiolite, Nord-Trøndelag, central Norwegian Caledonides

Lars-Petter Nilsson<sup>1</sup>, Leif Kero<sup>2</sup>, Rune Johansson<sup>2</sup>, David Roberts<sup>1</sup> & John Olav Mogaard<sup>3</sup>

<sup>1</sup> Geological Survey of Norway, PO Box 6315 Sluppen, N 7491 Trondheim, Norway.

<sup>2</sup> Geological Survey of Sweden, Box 670, SE 751 28 Uppsala, Sweden.

<sup>3</sup> Klostergata 78C, N 7030 Trondheim, Norway

Based on five profiles derived from helicopter-borne magnetic total-field data, modelling of the Raudfjellet ophiolite has confirmed the general geometry of the mafic-ultramafic complex, though with notable changes along strike from south to north. In the south, the mylonitic thrust zone of the ophiolite, according to modelled profiles 2, 3 and 4, dips regularly at 15-25° northwestwards, reaching a vertical depth of up to 800 m. In the north, modelling shows a more complex 3D picture of the magnetic body, there comprising both the large ultramafic (serpentinitic) block and the highly magnetic ultramafic-mafic cumulates of the overlying gabbroic block. Profile 5 shows an almost flat-lying, 1 500 m-long, prismatic body extending in depth to only 200-250 m. Profile 6, modelled WSW-ENE (i.e. with a 55° angle to profile 5), shows a high-magnetic, 1 000 m-long, nearly rhomb-shaped prismatic body, the footwall of which starts with a 35° dip and ends up with a dip of only 8° towards the southwest. This last body reaches a depth of up to c. 500 m in the southwest, and shows that the ophiolite is wedging out towards the northeast. This appreciable difference both in dip angles and depth ranges is considered to relate to well defined and strong magnetic anomalies where the latter are detected in the poorly exposed mafic block. The distribution of these anomalies is, in turn, inferred to be attributed to NW-SE-trending, strike-slip faults concealed beneath the extensive Quaternary deposits covering the western part of the ophiolite, which have thus resulted in segmentation of the complex.

## Introduction

The mafic-ultramafic complex exposed at and around Raudfjellet in Nord-Trøndelag, close to the Swedish border (Figure 1), was first reported over a century ago by Törnebohm (1896) and then mapped as diorite and serpentinite. A differentiation into peridotite, pyroxenite and gabbro came with the fieldwork and map-compiler work of Foslie (1959). Later mapping, by S. Bergman and H. Sjöström in 1988, as a contribution to a subsequent compilation of the preliminary 1:50 000 bedrock map-sheet 'Gjevsjøen' (Sjöström and Roberts 1992), provided a more refined picture of the complex on a modern topographic base, and discussions at that time favoured its subsequent interpretation as a dismembered and tectonically fragmented ophiolite (see Roberts 1997a). Subsequently, in a collaborative project between NGU and Statskog aimed at investigating the potential mineral resources within an extension of the Gressåmoen National Park, detailed mapping of the complex by NGU geologists in 1999-2000 led to the compilation of the geological map shown in Figure 2.

In a first description of the Raudfjellet ophiolite, Nilsson et al. (2005) distinguished two separate blocks – mafic and ultramafic – with an intervening, 4.5 km-long, hydrothermal zone comprising soapstone and overlying listvenite. The soapstone, with a talc content of 40-60%, was naturally of potential resource interest, and reconnaissance drilling of eight shallow holes, from 37 to 130 m in length, totalling 579 metres, was therefore carried out already in the winter of 2000. This shallow drilling was based on the first results from the 1999 field season (Nilsson et al. 1999), existing old airborne geophysical data (Håbrekke 1983), and also on the general 3D picture of the ophiolite fragment, dipping gently to the northwest, obtained from a cross-section accompanying the map by Sjöström and Roberts (1992). In the autumn of 2005, two ground-magnetic,

NW-SE test profiles were carried out across the ophiolite, including field measurements of magnetic susceptibility. As an interpretation of the acquired data proved to be unexpectedly difficult (see later), Statskog during the winter 2005/2006 raised funding for a new airborne survey. The entire ophiolite and subjacent rocks, altogether 30 km<sup>2</sup>, were covered with helicopter-borne, magnetic total-field and spectrometer measurements by NGU in March 2006. The resulting magnetic maps are shown here as Figures 4 and 5. The spectrometer measurements have not yet been compiled on maps. The complete magnetic dataset formed a basis for model calculations of the shape, thickness and extent of the complex at depth, carried out by two of the coauthors (Kero and Johansson 2006). The principal aim of this contribution is to present the main results of the geophysical profiling and resultant model for the mafic-ultramafic complex. Fuller details of the geology and structures are contained in Nilsson et al. (2005).

## Geological setting: a summary

Raudfjellet is situated south and west of the Grong-Olden Culmination (GOC), an antiformal structure crossing the main trend of the Caledonides (Figure 1) and exposing Late Palaeoproterozoic to Mesoproterozoic, felsic volcanites and granites (Troëng 1982, Roberts 1997a, b, Roberts et al. 1999). Two main Caledonian nappes constitute the GOC – the Olden Nappe and Formofoss Nappe Complex – each carrying a thin, low-grade, sedimentary cover of Ediacaran-Cambrian and possibly Early Ordovician age (Roberts 1997a). These two nappes form part of the Lower Allochthon of Scandinavian Caledonide tectonostratigraphy (Gee et al. 1985, Roberts and Gee 1985), and are succeeded by diverse nappes of the Middle Allochthon (e.g., Offerdal, Leksdal and Seve nappes). At Raudfjellet, the

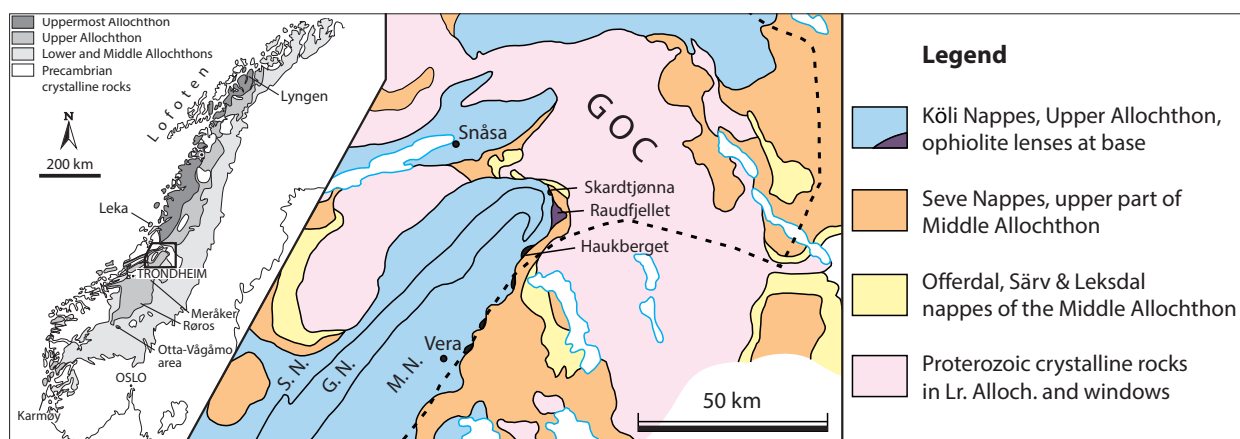


Figure 1. Simplified tectonostratigraphic map of the region in the vicinity of Raudfjellet. GOC – Grong-Olden Culmination; S.N. – Støren Nappe; G.N. – Gula Nappe; M.N. – Meråker Nappe.

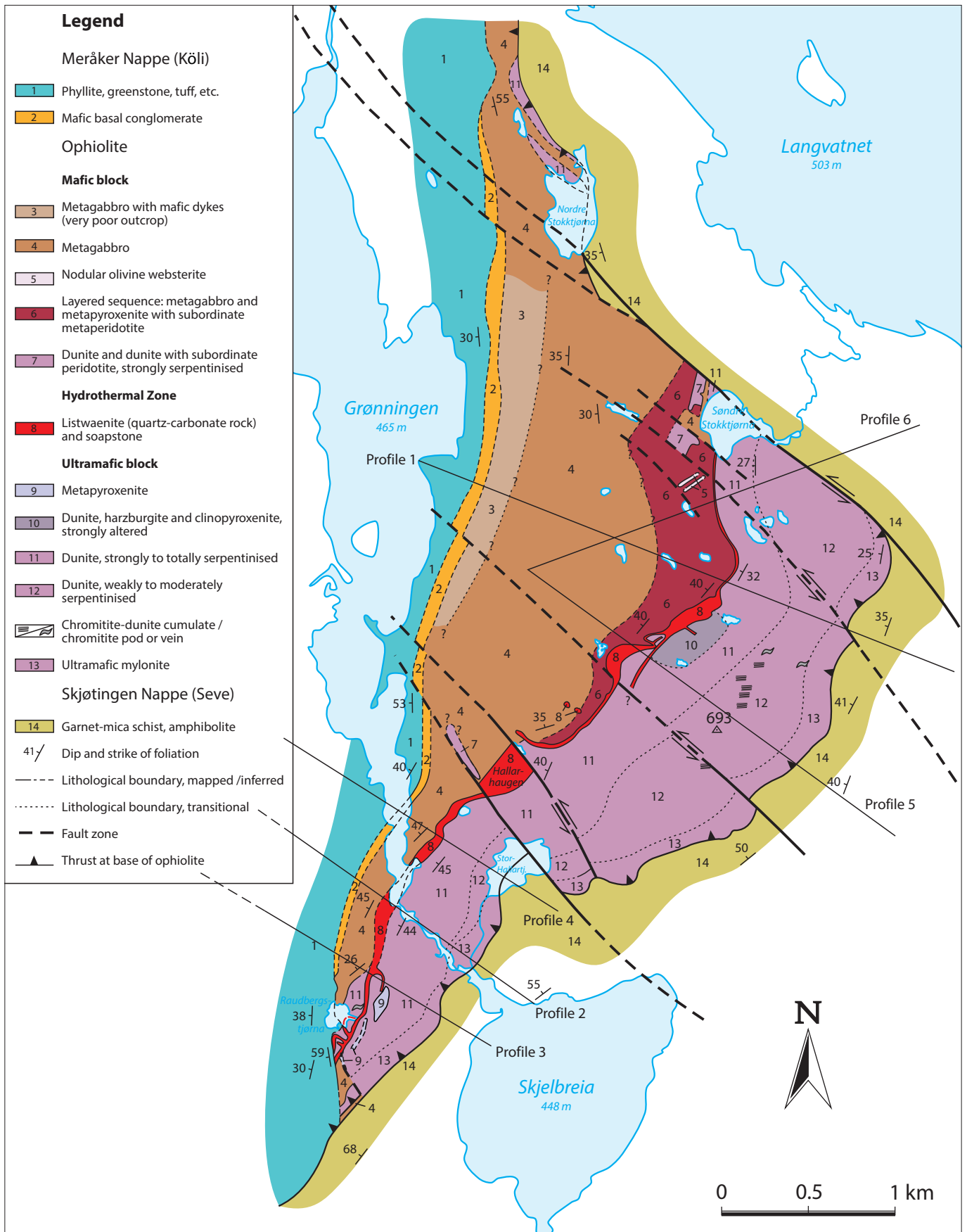


Figure 2. Geological map of the Raudfjellet ophiolite, modified from Nilsson et al. (2005), Sjöström and Roberts (2013) and including interpretations in poorly exposed areas based on the helicopter-borne magnetic map shown in Figure 4. Locations of profiles 2 to 6, extracted for modelling from helicopter-borne magnetic data, as well as the two ground-magnetic profiles 1 and 2, are also shown (profile 2 both ground and air-borne).

substrate to the ophiolite is represented by amphibolite-facies Seve rocks, known as the Skjøtingen Nappe in Mid Norway. The ophiolite itself is considered to form the basal part of one of the Köli nappes (Meråker Nappe), constituting the Upper Allochthon (mainly oceanic and arc terranes); and the ophiolitic rocks are unconformably overlain by a polymict conglomerate (Nilsson et al. 2005). Lenses of comparable ultramafic-mafic rocks, locally with an overlying conglomerate, occur along strike to the southwest (Figure 1), also at the base of the Meråker Nappe (Nilsson and Roberts, this volume). These lenses may link up with the fragmented Handöl ophiolite in the Tännfors area east of Storlien in Sweden (Bergman 1993). Further details of the regional geology are contained in the paper by Nilsson et al. (2005). In addition, a revised colour version of the 1:50 000 bedrock map-sheet 'Gjevsjøen' is now available (Sjöström and Roberts 2013).

## Raudfjellet ophiolite

### Pseudostratigraphy

The ophiolite fragment at Raudfjellet is partly dismembered consisting of a well preserved ultramafic lower part or block overlain by a hydrothermal zone comprising soapstone and listvenite which, in turn, passes up into a layered metagabbro and metapyroxenite. Above this is a massive, layered metagabbro with, higher up, mafic dykes intruding the gabbro. The assemblage is capped above an unconformity by a polymict conglomerate containing debris derived mostly from the ophiolite. At the very base of the ultramafic block there is a quite spectacular ultramafic mylonite. Details of the pseudostratigraphy have been documented in Nilsson et al. (2005). Here we present just a summary as a background for the geophysical profiling and modelling.

#### *The ultramafic block*

The basal mylonites reach up to c. 200 metres in surface width and carry lenses and thin layers of glassy ultramylonite, notably at the very base. The high-temperature, olivine and pyroxene mineralogy suggests that these tectonites are related to the obduction of the ophiolite. In places, the ultramafic mylonite rests on a thin, amphibolite-facies blastomylonite comprising material derived from the rocks of the subjacent Seve Nappe. The mylonites show abundant evidence of a younger, greenschist-facies, extensional reworking.

The ultramafites above the mylonites comprise essentially a single, cumulate dunite body up to c. 800 m in width and with substantial calculated thicknesses (see section on Model calculations where the mylonite zone and dunite body are combined), which is probably the largest such dunite known in the Scandinavian Caledonides. Minor bodies of clinopyroxenite/websterite are hosted by the dunite whereas distinct mantle peridotites (harzburgitic or lherzolite) seem to be totally absent

at Raudfjellet. Anastomosing, mylonitic shear zones pervade the lower parts of the body. Most of the central part is a homogeneous dunite with only modest serpentinisation, consisting of up to c. 90% olivine and only 10% serpentine by volume with accessory chromite where the dunite is least altered. In places there are minor occurrences of prominently layered, dunite-chromitite cumulates and also lenses of massive chromitite. Higher up in the dunite body, towards the northwest, serpentinisation increases and eventually the alteration is more or less complete. The serpentinised, homogeneous and completely non-stratified dunite (except for the above-mentioned very minor cases where cumulitic chromitite is involved) is interpreted to originate from the zone between overlying typical ultramafic cumulates (e.g. layered dunite-wehrlite) of the lower crust and underlying typical harzburgitic or lherzolitic mantle peridotites, though neither of these rocks is represented at Raudfjellet. In addition, it is conceivable that the Raudfjellet body might have been considerably larger in its original oceanic setting, since we can nowhere observe the contacts between the dunite and its original neighbouring rocks. In an accompanying paper (Nilsson and Roberts, this volume) we describe the difference between Raudfjellet and the next ophiolite fragment to the southwest, the Gaundalsklumpen - Haukberget fragment (Figure 1), where we interpret the ultramafic part of the latter as having derived from the mantle. It should also be emphasised here that there are several examples of ophiolites worldwide showing massive dunite bodies in the same size range and supposedly in the same position in a more general ophiolite stratigraphy as in Raudfjellet. The Thetford Mines Ophiolite, Quebec, Canada has, for example, an up to 500 m-thick dunitic zone confined to the crustal section of the ophiolite, sitting directly on top of the mantle peridotite tectonite (Schroetter et al. 2003).

#### *The hydrothermal zone*

The contact between the ultramafic and overlying mafic blocks is disjunctive and tectonic (Nilsson et al. 2005), but is also marked by a spectacular zone of hydrothermal alteration varying in thickness from 5 to 90 m. In general, this zone comprises soapstone at the base and listvenite above, both derivatives of CO<sub>2</sub> metasomatism. The soapstone has a talc content of 40-60% with magnesite as the other major constituent, and with dolomite and serpentine as subordinate minerals. Listvenite is essentially a magnesite-quartz rock that also contains dolomite, talc and chlorite, and traces of chromite.

#### *The mafic block*

Above the hydrothermally affected basal layers, mafic-ultramafic cumulates dominate in the high ground on Raudfjellet but are gradually cut out towards the southwest (Figure 2). The ultramafic cumulate layers are subordinate and impersistent, and are represented mostly by metapyroxenite and metaperidotite with sporadic layers of nodular olivine websterite. Within this modally layered unit, syn-magmatic erosional features

are seen locally. Above this complex cumulate unit there is a banded metagabbro that gradually gives way upwards into a massive metagabbro, which is the dominant rock type in the mafic block. In the higher parts, which are poorly exposed and heavily forested, the gabbro is transected by sporadic mafic dykes beneath the erosional top surface. Assuming that basaltic volcanites were once present at the top of this fragment of Early Palaeozoic ocean floor, as in the case of several other ophiolites in Mid Norway (e.g., Grenne et al. 1980, Furnes et al. 1988, Grenne 1989, Roberts et al. 2002, Slagstad 2003), in this particular case they have been removed by deep erosion prior to deposition of the unconformably overlying sedimentary succession.

#### Polymict conglomerate

Following obduction of the ophiolite, most probably in Early Ordovician time (Roberts et al. 2002, Nilsson et al. 2005), uplift, weathering and substantial erosion removed large parts, leaving an irregular surface upon which was deposited a polymict conglomerate. The unconformity at its base cuts down into deeper parts of the ophiolite pseudostratigraphy from north to south (Figure 2). Clasts, up to 35 cm in size, consist of subangular to subrounded ultramafic and mafic rocks with sporadic listvenite. The matrix is mostly dark grey-green, sand-size, ultramafic and mafic material (Nilsson et al. 2005).

#### Structural deformation

Away from the basal mylonites, a penetrative foliation is a fairly uncommon feature in the ultramafic block but becomes clearer in the metagabbro and layered gabbro/pyroxenite, where it is found to be steeper than the layering and axial planar to top-ESE asymmetrical folds. A fairly strong stretching and mineral lineation plunging c. WNW is prevalent in both blocks, and also in the mylonites. All in all, these structures clearly relate to top-ESE, contractional deformation and thrusting.

A greenschist-facies extensional reworking of the earlier, high-T fabrics is manifested in top-NW, extensional shear-bands in various parts of the ophiolite. Such structures are also common in the basal mylonites, although in this case mostly with a top-SW to WSW sense of shear. Transverse, NW-SE-trending, strike-slip faults are also recognised, notably in the northeast and in the vicinity of Stor-Hallartjern (Figure 2), first described by Sjöström and Bergman (1989). As we shall see later, other strike-slip faults are inferred to be present, judging from an analysis of the airborne magnetic data.

## Ground-magnetic profiling

### Introduction

In the autumn of 2005, two ground-magnetic test profiles were measured by NGU and Statskog in collaboration. Selection of the locations, directions and lengths of the two profiles was

based mainly on the contoured magnetic map from the 1982 helicopter-borne survey (map 1898/02 in Håbrekke 1983). This map shows an irregular and partly very strong, magnetic anomaly covering about half of the ophiolitic rocks at Raudfjellet. Various factors such as visual navigation, insufficient processing of the acquired data, as well as inadequate map compilation have together contributed to a magnetic contouring that did not give a correct (in detail) magnetic picture of the complex but still good enough to obtain a rough impression of what caused the anomaly pattern.

In general, it was considered that the ultramafic block (Figure 2), made up essentially of strongly serpentinised dunite with a high content of secondary magnetite, was the major contributor to the anomaly. The mafic block, essentially composed of massive gabbro, was considered to be mainly non-magnetic (i.e. paramagnetic). Such a simple two-fold model where the main rocks involved show very large contrasts in magnetic susceptibility (on average, about two orders of magnitude), would be ideal in order to obtain an accurate dip angle as well as an indication of the possible depth range of the hydrothermal zone. This is because the hydrothermal zone follows conformably on top of the moderately northwest-dipping, highly magnetic, serpentinite body. At the same time, the hydrothermal zone is situated directly in the footwall of low-magnetic gabbro southwards from Hallarhaugen. The latter would then not mask or hide the hydrothermal zone. This simple model was shown to work in broad terms, but with some unexpected complications and deviations as shown below in the section: Observations along the profiles following the Instrumentation section.

### Instrumentation, execution of measurements, data acquisition and monitoring

The ground profiling was conducted by Rolf Lynum (RL) and Lars-Petter Nilsson (LPN) from NGU and Asbjørn Flaar (AF) from Statskog on the 19<sup>th</sup> and 20<sup>th</sup> of September, 2005. The magnetic total field was measured with NGU's portable *Scintrex Envi-Mag (serial No. 9310049)* magnetometer, and positioning in UTM-coordinates was determined with a *Garmin eTrex* GPS.

As the first member in the surveying crew, AF laid out profile directions with sticks and compass and measured out 50 m distances with a measuring wire. At every 50 m interval, a waypoint (WP) was registered with the GPS. Between the waypoints, measuring points were paced out for every c. 10 m. As the second member in the crew, RL measured the magnetic total field and logged the UTM-coordinates both of the WPs and the intervening measuring points. As the last in the group, LPN carried the GPS in order to prevent any influence on the magnetic measurements. The magnetic total-field readings (plus a recorded value for magnetic noise) and the GPS positions were recorded in their respective instruments together with the exact time of the readings. In addition, the total-field readings and WP-coordinates were manually logged by LPN for back

up. Furthermore, LPN observed and recorded bedrock outcrops along the profiles as well as measuring magnetic susceptibility at selected locations using a hand held *Microkappa (Model KT-5)* from Geofyzika Brno with a quoted detection limit of  $1 \times 10^{-5}$  SI (cf. Table 1). The instrument is based on electromagnetic induction in an air-filled coil with a diameter of 55 mm.

After returning to NGU, the accumulated data from the magnetometer and GPS, well synchronised, were downloaded and tabulated. The measured data were later compared with data for magnetic storms/disturbances recorded at the magnetic base station at Rørvik, Nord-Trøndelag. The readings from the Rørvik base station showed that no magnetic disturbances had occurred during the actual field days.

## Helicopter-borne magnetic survey

The helicopter-borne survey in Raudfjellet was carried out in connection with an exploration survey in the neighbouring Skjækerdalen area (Mogaard 2006). The measuring and positioning instrumentation, operating conditions, data acquisition and processing, and finally map production were basically the same in the two assignments. The data below are therefore mostly extracted from the Skjækerdalen report.

The area surveyed at Raudfjellet is a rectangular area measuring  $5 \times 6$  km, with longest side of the rectangle oriented approximately NE-SW ( $041^\circ$ ). The distance flown and areas covered are approximately 300 line-km and  $30 \text{ km}^2$ .

**Table 1.** Magnetic susceptibility measured using a hand-held *Microkappa Model KT-5* on outcrops along the ground-magnetic profile 1. Values are given in SI-units  $\times 10^3$ , detection limit as quoted by instrument manufacturer Geofyzika Brno is  $1 \times 10^{-5}$  SI-units.

| lithology                  | phyllite*    | gabbro** | pyroxenite-melagabbro† | pyroxenite†† | dunite‡ | amphibolite‡ | garnet-micaschist‡ |      |
|----------------------------|--------------|----------|------------------------|--------------|---------|--------------|--------------------|------|
| top-to-bottom              | hanging-wall |          |                        |              |         |              | footwall           |      |
| number of outcrops         | 1            | 1        | 3                      | 4            | 16      | 1            | 5                  |      |
| arithmetic mean            | 0.37         | 0.30     | 0.34                   | 56.0         | 51.2    | 0.56         | 1.42               |      |
| standard deviation         | 0.16         | 0.06     | 0.09                   | 20.7         | 11.6    | 0.20         | 1.74               |      |
| median                     | 0.37         | 0.29     | 0.36                   | 54.5         | 50.4    | 0.58         | 0.62               |      |
| maximum value              | 0.65         | 0.40     | 0.49                   | 89.7         | 92.0    | 0.75         | 6.77               |      |
| minimum value              | 0.19         | 0.22     | 0.16                   | 16.5         | 30.2    | 0.36         | 0.03               |      |
| number of values (n)       | 12           | 13       | 26                     | 17           | 46      | 3            | 20                 |      |
| individual measured values |              |          |                        |              |         |              |                    |      |
|                            | 0.36         | 0.24     | 0.40                   | 78.4         | 44.7    | 60.8         | 0.36               | 0.21 |
|                            | 0.19         | 0.22     | 0.38                   | 54.5         | 60.7    | 52.0         | 0.75               | 0.06 |
|                            | 0.21         | 0.27     | 0.45                   | 66.4         | 40.5    | 63.5         | 0.58               | 0.32 |
|                            | 0.42         | 0.33     | 0.38                   | 53.7         | 41.3    | 50.4         |                    | 0.12 |
|                            | 0.23         | 0.29     | 0.48                   | 34.7         | 42.6    | 54.4         |                    | 0.03 |
|                            | 0.61         | 0.35     | 0.35                   | 89.7         | 50.4    | 72.8         |                    | 0.03 |
|                            | 0.53         | 0.40     | 0.35                   | 63.9         | 42.9    | 60.3         |                    | 1.61 |
|                            | 0.28         | 0.35     | 0.41                   | 47.0         | 51.2    | 71.3         |                    | 4.06 |
|                            | 0.37         | 0.32     | 0.43                   | 86.6         | 48.0    | 41.5         |                    | 2.36 |
|                            | 0.24         | 0.22     | 0.40                   | 78.2         | 45.4    | 49.5         |                    | 2.70 |
|                            | 0.39         | 0.40     | 0.42                   | 64.7         | 63.6    | 51.5         |                    | 1.11 |
|                            | 0.65         | 0.29     | 0.40                   | 23.0         | 52.9    | 50.7         |                    | 2.25 |
|                            |              | 0.28     | 0.49                   | 47.8         | 38.2    | 52.0         |                    | 3.46 |
|                            |              |          | 0.38                   | 54.9         | 35.2    | 59.0         |                    | 6.77 |
|                            |              |          | 0.16                   | 50.3         | 48.7    | 42.4         |                    | 0.41 |
|                            |              |          | 0.18                   | 16.5         | 39.9    | 46.1         |                    | 0.64 |
|                            |              |          | 0.27                   | 41.2         | 50.2    | 54.1         |                    | 0.55 |
|                            |              |          | 0.26                   |              | 30.2    | 92.0         |                    | 0.52 |
|                            |              |          | 0.32                   |              | 64.6    | 43.2         |                    | 0.62 |
|                            |              |          | 0.19                   |              | 53.1    | 40.6         |                    | 0.61 |
|                            |              |          | 0.21                   |              | 48.4    | 54.7         |                    |      |
|                            |              |          | 0.23                   |              | 72.4    | 53.2         |                    |      |
|                            |              |          | 0.32                   |              | 32.6    | 42.9         |                    |      |
|                            |              |          | 0.27                   |              |         |              |                    |      |
|                            |              |          | 0.36                   |              |         |              |                    |      |
|                            |              |          | 0.26                   |              |         |              |                    |      |

The listed lithologies represent a sequence from hanging-wall at: \* Meråker Nappe, Furuhattangen; \*\* massive, isotropic; † paramagnetic/layered; †† ferromagnetic/layered; ‡ partly or totally serpentinized; until ‡ Seve, which is the footwall.

## Survey topographic and magnetic conditions

The topography is fairly moderately undulating in the survey area with 226 m between the highest and lowest points in the terrain. The terrain is partly vegetated with open forest and intervening areas of exposed bedrock. We are not aware of any reported discrepancies from the  $30 \pm 10$  m nominal ground clearance for the 'bird' (the magnetometer) during the survey.

Diurnal changes in the Earth's magnetic field affect magnetic data. At the magnetic base station (in Verdalen), no magnetic storms or other abrupt variations in the Earth's magnetic field that could have affected the magnetic data were recorded during the survey period.

## Data acquisition

The survey aircraft was an *Aérospatiale Écureuil AS 350 B-2*. The flying speed was approximately 100 km per hour (28 metres per second). Flight lines were flown in alternating directions at headings of  $13^\circ$  and  $311^\circ$  with a nominal flight line spacing of 100 m. A 5-frequency EM system and the magnetometer were enclosed in a 6-m long 'bird' suspended by cable 30 m below the helicopter (the EM-data were also collected, but not processed in the Raudfjellet assignment). The nominal flying height was 60 m above ground level (AGL).

NGU personnel responsible for data acquisition were John Olav Mogaard and Janus Koziel. The pilot from HELITRANS AS was Jens Fjelnset.

### *Magnetic measurements*

A *Scintrex CS-2 cesium* vapour magnetometer was used. The magnetometer resolution is 0.01 nT. The sampling rate was 10 measurements per second (approximately 3 m spacing).

A *Scintrex ENVI-mag* proton precession magnetometer was located at the base in Verdalen, and was used for base station measurements. The base station magnetometer was synchronised with the Scintrex magnetometer in the helicopter to ensure proper removal of diurnal magnetic changes from the helicopter magnetic measurements. The magnetic total field at the base station was digitally recorded during flights every third second.

### *Navigation, altimetry and data logging*

The navigation system used is an *Ashtech G12*, 12 channel receiver. Position accuracy using this system is better than  $\pm 5$  m. The navigation console is a *PNAV 2001* manufactured by the Picodas Group Ltd, Canada. Profile line data are entered into the console and are displayed on a left/right-display on the console. The pilot can see his position with respect to these pre-defined lines and make adjustments accordingly.

The helicopter is equipped with a *King KRA-430* radar altimeter measuring height above ground level. The altimeter data are recorded digitally and altitude is displayed in front of the pilot. The altimeter is accurate to 5 percent of the true flying height.

## Processing and map preparation

The data were processed at the Geological Survey of Norway in Trondheim using Geosoft processing software (Geosoft Oasis Montaj 6.2, 2005). Obvious inaccuracies in navigation were manually removed from the data. The datum used was WGS84 and the projection was UTM zone 33.

Total field magnetic data: The data were inspected flight-by-flight and any cultural anomalies were identified and manually removed. A base station correction was applied to each flight using corrections based on diurnal measurements from the base station magnetometer at the base in Verdalen. Finally, a time lag of 0.6 sec (6 points) was applied to the base-mag corrected (levelled) magnetic data.

A total magnetic field map in scale 1:20 000 was produced using a grid cell size of  $25 \times 25$  metres.

## Model calculation

A model calculation based on the helicopter-borne magnetic measurements was performed in 2006 by Kero and Johansson (op. cit.). From the gridded total magnetic intensity dataset, five profiles were extracted for modelling by means of the modelling software Potent (Geophysical Software Solutions 2005). The locations of the profiles are shown in Figures 2, 4 and 5.

### Magnetic properties

The Earth's magnetic (inducing) field in the area has a total intensity of 50 000 nT, a declination  $0^\circ$ , and an inclination of  $73^\circ$ .

Based on susceptibility measurements, the indicated magnetic bodies have an assumed susceptibility of approximately 0.05 SI units. However, initial modelling results showed that magnetic bodies with the above, assumed susceptibility cannot explain the measured anomalies. Therefore, it became clear that the investigated magnetic bodies must also be characterised by a certain degree of remanent magnetisation. In order to achieve a good fit between the measured and the calculated anomalies, a remanent magnetisation of 1.5 A/m has been assumed for profiles 2-5 and 2.0 A/m for profile 6. The direction of the remanent magnetisation is assumed to be in alignment with the present direction of the Earth's magnetic (inducing) field.

The assumed properties are very realistic if compared to known properties of similar magnetic rocks but it must be emphasised that, in the case of Raudfjellet, only the magnetic susceptibility value used for modelling is based on actual measurements within the investigated area.

## Observations along the ground-magnetic profiles (Figure 3)

### *Profile 1*

Profile 1, 3 370 m long, measured in the direction  $109^\circ$  and with 10 m spacing between each measuring point, extends from

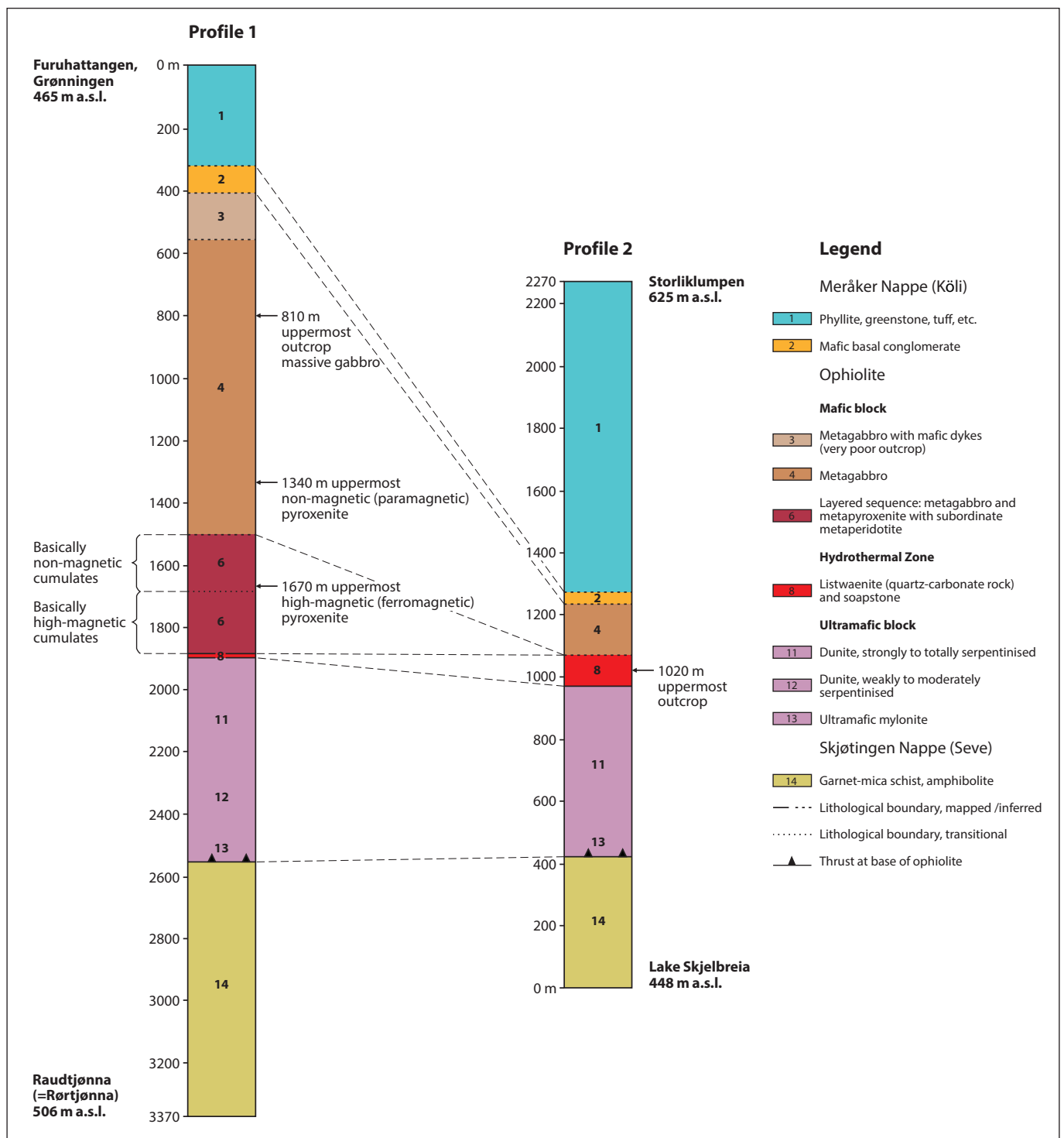


Figure 3. Geology drawn as columns along two ground-magnetic profiles, 1 and 2, across the Raudfjellet ophiolite. Locations of the profiles are shown in Figure 2. Profile 1 was measured from NW to SE; profile 2 from SE to NW. Bedrock observations are indicated as well as a geological correlation between the two profiles.

the point Furuhattangen at the shore of lake Grønningen in the northwest to the tarn Raudtjønnå in the southeast across the northern and supposedly thickest part of the ophiolite fragment (Figure 2). The profile starts in non-outcropping Köli metasedimentary rocks and after about 500 m passes into massive gabbro that continues for about 1 500 m along the profile. The first outcrop encountered is massive gabbro at 810 m from

the start of the profile. From c. 1 500 m, the gabbro gradually changes character from massive to layered gabbro including also subordinate leucogabbro/anorthosite and accompanied by an increasing number of ultramafic layers stratigraphically downwards (see stratigraphic column in Figure 3). The first ultramafic layers encountered along the profile at 1 340 m are non-magnetic (i.e. paramagnetic) pyroxenite in massive gabbro,



but later also high-magnetic (i.e., ferromagnetic) pyroxenite and peridotite layers were encountered from 1 670 m. The number of ultramafic layers is increasing downwards towards the contact with the hydrothermal zone at 1 890 to 1 900 m. As a whole, we may regard the 180 metres between 1 500 and 1 680 m as basically non-magnetic cumulates and the 220 m between 1 680 and 1 900 m as high-magnetic cumulates of the mafic block. The latter will then contribute to masking the here thin and non-magnetic hydrothermal zone situated just below these cumulates. At the southeastern side of the hydrothermal zone, the large, monotonous serpentinite/metadunite body (the main constituent of the ultramafic block) is passed (over a distance of c. 650 metres) before we enter the poorly exposed, low-magnetic, Skjøtingen (Seve), footwall mica schists with minor amphibolites at c. 2 550 m and continue on the last c. 820 m-long portion of the profile down to the shore of Raudtjønnna.

An unexpected phenomenon was encountered along this profile. Some of the ultramafic pyroxenitic and peridotitic layers in the mafic block were shown to be strongly magnetic with measured total field values along the profile up to 54 083 nT with a corresponding magnetic susceptibility of  $61 \times 10^{-3}$  SI. These values are almost equal to even the highest total field values obtained when profiling over the large serpentinite body (max. 54 405 nT and corresponding  $56 \times 10^{-3}$  SI). The profile section with high-magnetic cumulates occurring between 1 680 and 1 890 m were inserted as a separate high-magnetic body in the interpretation of the profile (Figure 6). In this way, the non-magnetic hydrothermal zone came to be intercalated between the two high-magnetic blocks.

Anomalous negative spikes with values down to -7 000 nT are regarded as noise and have been removed from the profile (Figure 6). The results from the airborne measurements showed no sign of local magnetic minima in the area.

#### *Profile 2*

Profile 2, 2 270 m long, measured in the direction  $300^\circ$ , and also with 10 m between each measuring point, started in the southeast at the shore of lake Skjelbreia well into the Skjøtingen (Seve) nappe footwall of the ophiolite (Figure 2). The profile then passed through the high-magnetic serpentinite body between 420 and 970 m, crossed soapstone and listvenite of the hydrothermal zone between 970 and c. 1 070 m, then the massive gabbro which has here thinned very much between c. 1 070 and c. 1 220 m; and finally traversed low-grade Köli phyllites, etc., over the last kilometre up to the crest of the hill Storliklumpen at 620 m. asl. (Figure 6). The last outcrop observed was of listvenite at the shore of lake Grønningen at 1 020 m, i.e. only half-way along the profile. Along the last 1 250 m of profile 2 no outcrops were observed, thereby making interpretation of this particular magnetic profile more difficult. Very little noise was recorded along this profile as compared with profile 1. A single c. 1 000 nT sudden drop in total field occurred in the border zone between serpentinite

and soapstone/listvenite near the outlet of lake Grønningen. On the other hand, the high values measured above the serpentinite body did not fall off as soon as expected when entering into the non-magnetic hangingwall rocks to the serpentinite (first the hydrothermal zone, then massive gabbro of the ophiolite and finally the overlying Köli phyllites). In fact, the measured total field values did not diminish much at all, remaining remarkably high and stable, and falling only from c. 52 200 nT at 1 200 m to c. 51 900 nT at 2 270 m at the end point Storliklumpen. This hill is situated at c. 1 000 metres into the phyllites and associated rocks lying above the ophiolite and is, in addition, 155 m higher than lake Grønningen with the last outcrops consisting of serpentinite and listvenite. The measured total field values thus necessitated a very gently northwest-dipping surface of the large serpentinite body for a best possible curve fit when modelling the profile (Figure 6). This unexpectedly low angle of dip (c.  $<5-10^\circ$ ) did not fit at all with dips measured on the surface near the outlet of lake Grønningen and in the surrounding terrain (c.  $25-45^\circ$  dip angles), nor with the information obtained from the nearest drillholes (Dh 2 and 7, Nilsson 2000).

Due to the problems of properly explaining these quite unexpected measuring results and the very shallowly dipping body modelled from the readings, Statskog decided not to continue further ground profiling. Instead they decided to carry out a new airborne survey to obtain a better overview of the whole area in a wider context.

## Modelling results from the helicopter-borne magnetic survey

### Total magnetic field and magnetic vertical derivative maps

The total magnetic field map in Figure 4 shows a great number of interesting magnetic anomalies, both larger structures and smaller features, clear linear structures and some quite irregular ones. Foremost, a number of very large and strong positive anomalies, as well as complementary negative ones, occur within and along both the ultramafic and the mafic block of the ophiolite. Since the map, however, was financed and compiled in connection with the ongoing exploration for talc/soapstone and magnesite, focus was placed on the magnetic trace and signature of the hydrothermal zone and its immediate and concordant substrate, i.e. the large serpentinite body of the ultramafic block. Many of the other, new and interesting anomalies have therefore so far been left out and not followed up in the field. This applies, for example, to the many small and very strong 'point anomalies' within the lower, cumulitic part of the mafic block where thin and impersistent, high-magnetic, pyroxenite layers (ferropyroxenites) alternate with gabbroic cumulates. The large, NW-SE-trending, negative anomaly in the midst of the massive gabbro unit (i.e., where the mafic block is expected to be at its thickest) on the east side of

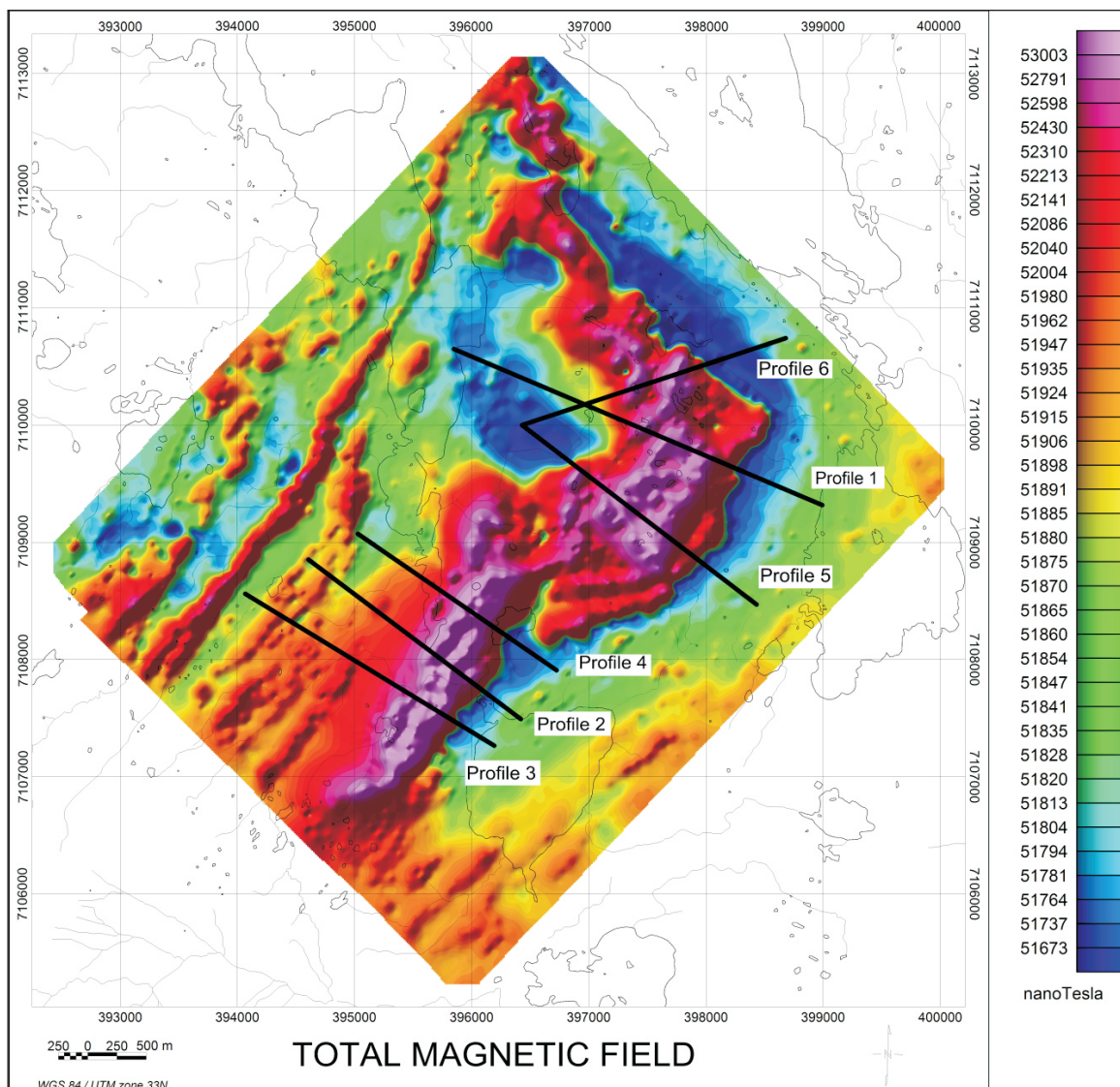


Figure 4. The total magnetic field measured from the helicopter. The intensity of the total magnetic field is given in nanoTesla. The locations of the five profiles (2 to 6) extracted for the modelling are shown together with profile 1.

lake Grønningen is located in an unexposed area devoid of any outcrops, and it is therefore still unknown to us what it really represents. Whatever the causes, the individual anomalies in the new aeromagnetic map may serve as a very good basis for any future detailed field study of the ophiolite fragment. The same applies to the magnetic vertical derivative map in Figure 5. This map especially enhances internal structures in the metadunite ultramafic block (Figure 2). The anomaly pattern seems to have been caused mainly by the strong tectonic fragmentation of the body, and in addition possibly by substantial variations in the degree of serpentinisation of the precursor dunite. Based on the new aeromagnetic maps, the first author (LPN) suggested modelling the geology along four new profiles plus the old profile 2 discussed above. The modelling work was carried out by two of the present coauthors (Kero and Johansson 2006).

### Modelling results from the southwestern area (Figure 7, profiles 2-4)

The modelling of the southwestern part of the survey area (profiles 2-4, Figure 7) shows a sheet-like magnetic body with a convex upper surface and flat, inclined base dipping at c. 40° to the northwest. The sheet has a maximum thickness of approximately 200 m and a length of 2 km, and it reaches a depth of at least 1 200-1 500 metres below the ground surface. The depth extent is actually a minimum value since the model can be extended farther down without causing any significant change in the calculated anomaly at the surface. The base of the sheet appears to correspond with the down-dip extension of the thrust fault exposed and mapped on the topographic surface. The modelling shows that the northeastern edge of the sheet dips to the northeast.

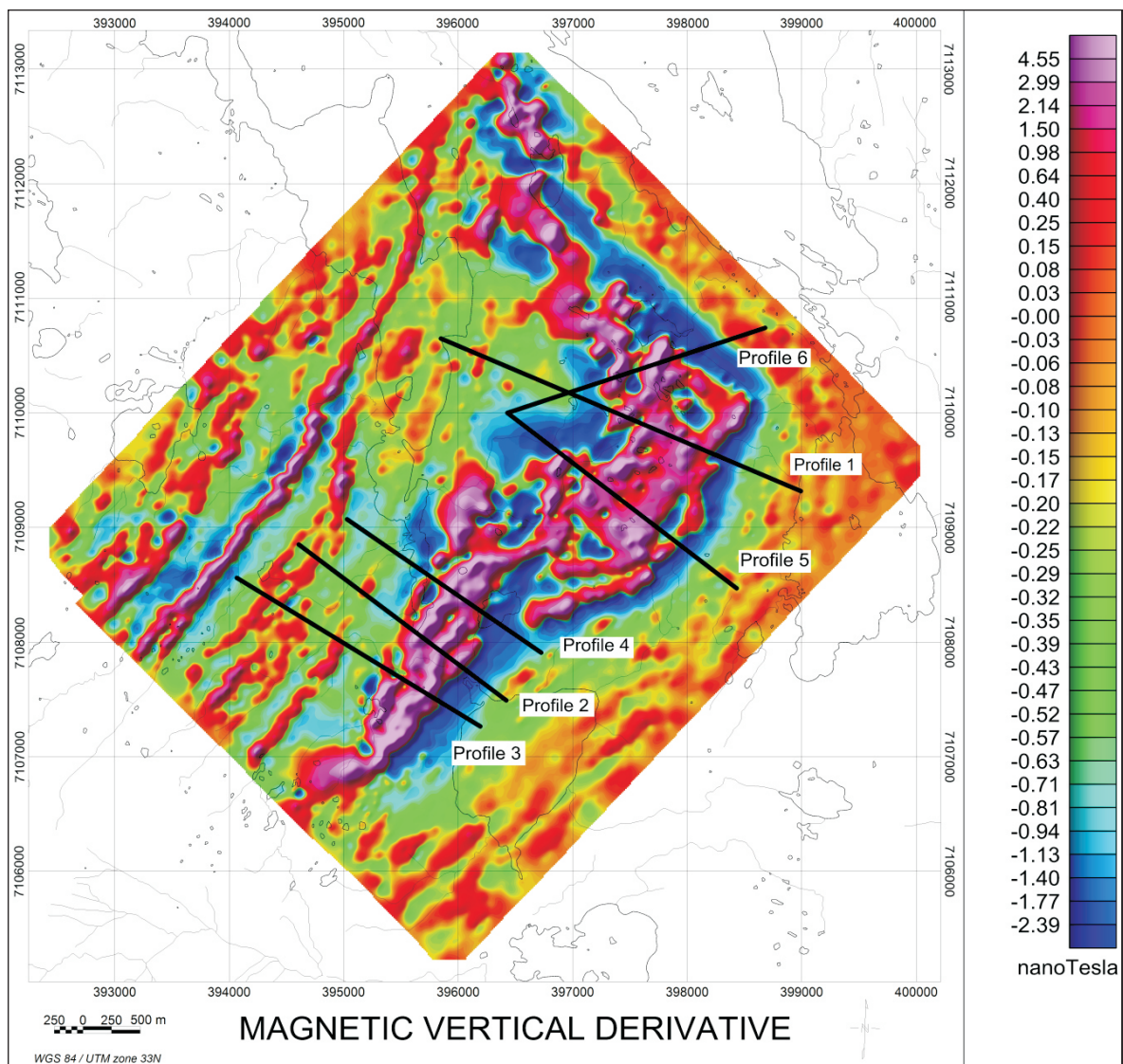


Figure 5. The magnetic vertical derivative with values given in nanoTesla. The locations of the five profiles (2 to 6) extracted for the modelling are shown together with profile 1. The anomaly pattern is enhancing the internal structures in the ultramafic (metadunitic) block.

The main anomaly displays a number of ‘internal peaks’, a feature which suggests that the simple sheet model could possibly be replaced by a series of thin sheets with varying susceptibility and/or remanent magnetisation. However, the modelling shows that the magnetic pattern could just as well be explained by the magnetic body having an irregular form near the surface, or even by topographic effects. A more detailed analysis of the internal structure of the magnetic body would require the acquisition of far more detailed magnetic data. Measurements of magnetic susceptibility along the ground-magnetic profile 1 varied, for example, between 0.03 and 0.09 SI units (46 individual field measurements distributed at 16 locations along the profile, and the values varied very irregularly along the profile); see Table 1.

It should be added that chemical analyses of metadunite samples verify substantial local variations in the content of serpentine,

i.e. the content of serpentine vs. olivine (cf. Nilsson 2000, fig. 20 and table 7). When olivine is transformed to serpentine, the latter is accompanied by significant amounts (several wt.%) of very fine-grained, disseminated, secondary magnetite. This is the mineral contributing to the magnetic body/bodies causing the positive magnetic anomaly/anomalies here in question. The nature of the apparent remanent magnetisation is not yet clear.

#### Modelling results from the northeastern area (Figure 7, profiles 5- 6)

The anomalous pattern in the northeastern part of the area (profiles 5 and 6) is more complex than in the southwest (Figure 7). The apparent geometry differs quite significantly between the two profiles. A reasonable fit with the measured data requires a more pronounced contribution from remanent magnetisation

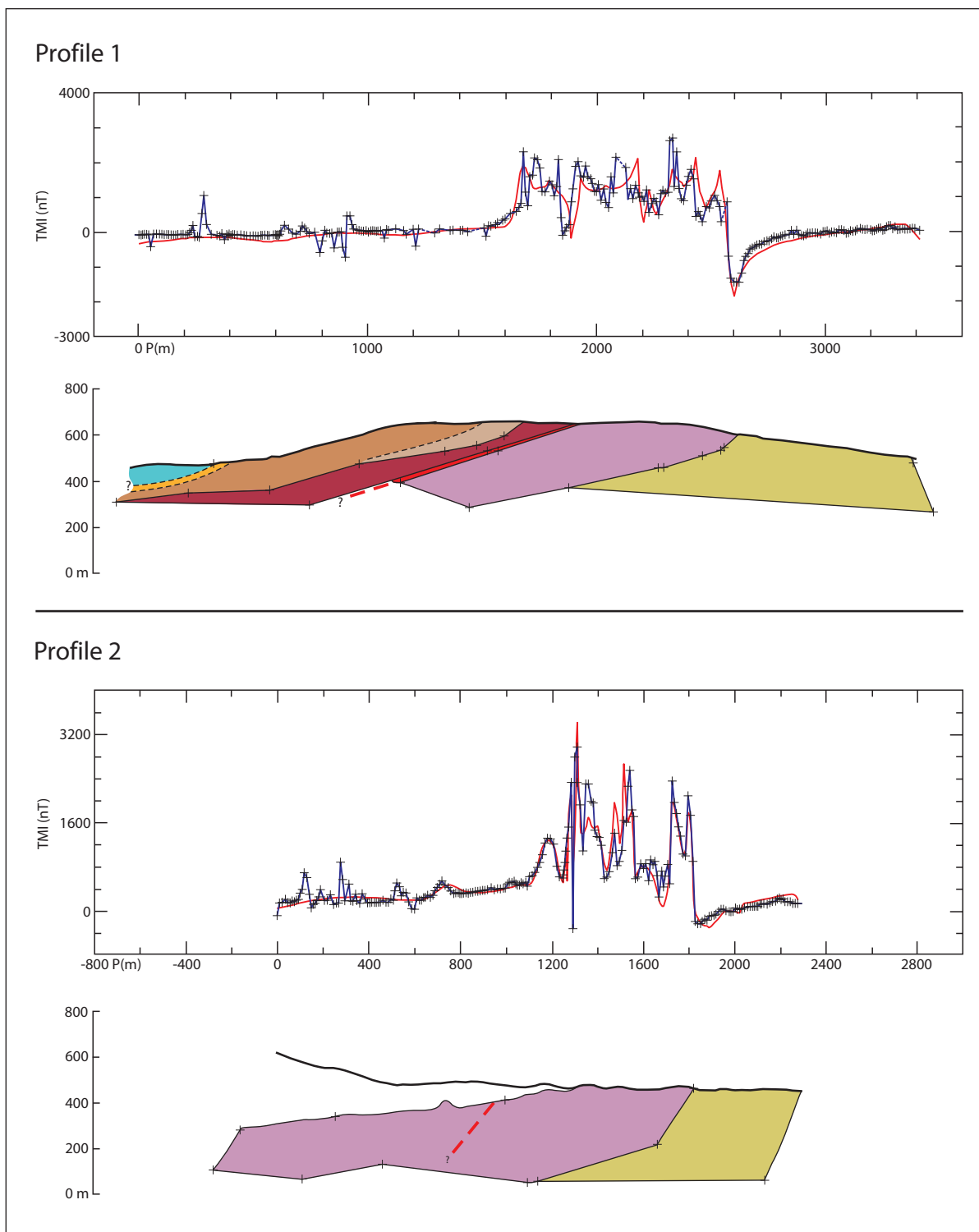


Figure 6. Modelling of profiles 1 and 2 based on ground-magnetic measurements. The blue line represents the measured magnetic field, the red line the theoretical response from the model. Colouring of the bodies is in accordance with that shown on the geological map in Figure 2 and the columns in Figure 3. A number of local, deviant readings lower than -1 000 nT caused by instrument disturbances have been deleted from the graph of profile 1.

as compared to the profiling in the southwestern part of the investigated area. Again, internal variations have been neglected when modelling the magnetic body.

Profile 5 (Figure 7) displays a sheet-like, almost lenticular,

approximately horizontal magnetic body with a length/thickness ratio of c. 3:1. The thickness of the sheet is 200-300 m and its upper, outermost contacts dip outwards, i.e., towards NW in the northwest and towards SE in the southeast.

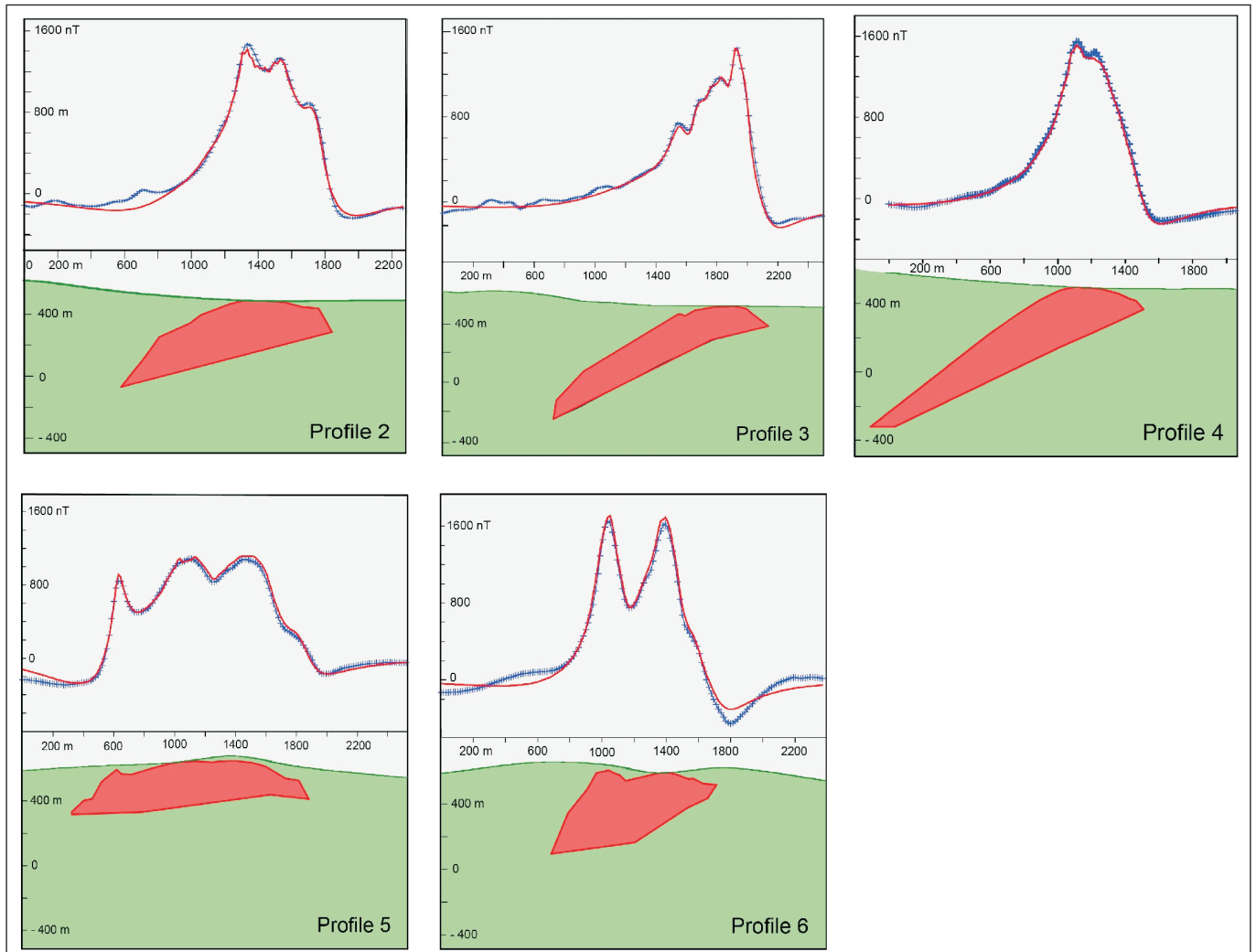


Figure 7. Modelling of the helicopter-borne data from Raudfjellet. The blue line represents the measured magnetic field, the red line the theoretical response from the model. Profile locations are shown in Figures 2, 4 and 5. For magnetic properties of the Earth's magnetic field and the assumed properties of the anomalous magnetic body, see text.

Profile 6 (Figure 7) also shows the body to have a sheet-like form although it is shorter, thicker and more stunted than in Profile 5. The overall dip is c.  $45^\circ$  to the southwest, but again there is a tendency to show outward dips (SW and NE, respectively) close to the surface. The vertical cross-section is rhombic in shape (edge length approximately 600 m), suggesting that the magnetic body can be interpreted to have a sheet-like form with very limited depth extension. Although the interpreted depth extension is comparatively poorly resolved, it is nevertheless obvious that the depth extent of the body is far more limited than in the southwestern area. An alternative interpretation would be that the thickness of the sheet decreases dramatically with depth.

## Discussion

The helicopter-borne, magnetic total-field data presented here have indicated that the relatively simple picture of the

subsurface form of the c. 9 km<sup>2</sup> Raudfjellet ophiolite reported earlier (Nilsson et al. 2005) requires some modification. The magnetic anomaly pattern strongly indicates that NW-SE-trending, steep to vertical, strike-slip faulting has segmented the ophiolite in a way not readily recognised during the earlier surface bedrock mapping, especially in the largely unexposed and forested areas of the mafic block in the west (cf. Figures 2 and 4). The ophiolitic complex and its neighbouring Seve and Köli metasupracrustal rocks show markedly different magnetic properties. The ophiolitic rocks as a whole contain either abundant magnetite (the only ferromagnetic mineral present in significant amounts) or only paramagnetic and diamagnetic minerals.

Based on five profiles derived from helicopter-borne magnetic total-field data (Figure 4), modelling of the Raudfjellet ophiolite has confirmed the general geometry of the mafic-ultramafic complex, though with notable changes along strike from south to north (Figure 7). The modelled profiles 2, 3 and

4 show a large ultramafic body of variably serpentinised dunite dipping regularly at 30-40° (hanging-wall side of the body) towards northwest for at least 1 200 to 1 500 m in the southern half of the ophiolite, thus corresponding to a vertical depth of 600-800 m. The footwall of this high-magnetic modelled body, which represents the mylonitic thrust zone of the ophiolite, dips regularly at 15-25° northwestwards.

In the northern half, however, i.e., to the north of the distinct Hallarhaugen fault-bound segment, the regular pattern seen in the south is markedly disrupted. Modelling here shows a more complex 3D picture of the magnetic body which includes both the large ultramafic (serpentinitic) block and the highly magnetic, ultramafic-mafic cumulates (ferropyroxenites) of the overlying mainly gabbroic block. Profile 5 shows an almost flat-lying, 1 500 m-long, prismatic body with a depth range in the order of only 200-250 metres. The hanging-wall side of this prism is dipping at c. 45° towards the northwest. Profile 6, modelled WSW-ENE (i.e. with a 55° angle to profile 5), shows a high-magnetic, 1000 m-long, nearly rhomb-shaped prismatic body, the footwall of which starts with a 35° dip and ends up with a dip of only 8° towards the southwest. The depth range of this last body is up to 500 m in the southwest, and further shows that the ophiolite is wedging out towards the northeast. The hanging-wall side of this rhomb-shaped body is dipping at c. 60° towards the southwest. This abrupt change in the depth extension of the modelled magnetic body occurring around Hallarhaugen may be explained by the prominent strike-slip faulting of the ophiolite, which has resulted in extensive block faulting and segmentation of the complex.

The observed rapid changes between thin, highly magnetic, ferropyroxenite layers and low-magnetic gabbro layers in the lower, cumulitic parts of the mafic block (Figures 3 and 6) proved to be difficult to deal with in the final modelling. This was due to both the limited amount of geophysical field data available for the modelling and the scarcity of geological information within the poorly exposed, lower, layered portion of the mafic block. The relatively thin and impersistent ferropyroxenite layers, each one in itself a quite insignificant tabular body compared to the size of the serpentinised dunite block, were therefore ultimately included in the one, single, highly magnetic body that constitutes the basis for the model calculations.

To resolve the various components of the 'ultramafic block' and the layered sequence of metagabbro-metapyroxenite would require far more detailed geophysical data and would furthermore, to be reliable, have to be confirmed by drilling. Should further investigations be made at some future date, the present geological information and geophysical modelling results will nevertheless provide a good basis for the planning of the work.

### Acknowledgements

We are indebted to the referees Tore Prestvik (geology) and Odleiv Olesen (geophysics) who suggested several additions which led to improvements in the final manuscript. We also thank Torleif Lauritsen for preparing the maps in Figures 4 and 5, and Irene Lundquist for skilful drafting of figures. Asbjørn Flaatt and Rolf Lynum are thanked for assistance with the ground profiling. Asbjørn Flaatt further provided accommodation and transport in the field.

## References

- Bergman, S. (1993) Geology and geochemistry of mafic-ultramafic rocks (Köli) in the Handöl area, central Scandinavian Caledonides. *Norsk Geologisk Tidsskrift*, **73**, 21-42.
- Foslie, S. (1959) Geologisk kart JÆVSJØEN (Rektangel 51C), M 1:100 000. *Norges geologiske undersøkelse*.
- Furnes, H., Pedersen, R.B. and Stillman, C.J. (1988) The Leka ophiolite complex, central Norwegian Caledonides: field characteristics and geotectonic significance. *Journal of the Geological Society of London*, **145**, 401-412.
- Gee, D.G., Kumpulainen, R., Roberts, D., Stephens, M.B., Thon, A. and Zachrisson, E. (1985) Scandinavian Caledonides, Tectonostratigraphic Map, 1:2 million. In Gee, D.G. and Sturt, B.A. (eds.) *The Caledonide Orogen – Scandinavia and related areas*. John Wiley & Sons, Chichester.
- Geophysical Software Solutions (2005) Potent reference Manual. *Geophysical Software Solutions Pty. Ltd., Canberra*, 108 pp.
- Geosoft (2005) OASIS Montaj v 6.2 Mapping and processing system. The core software platform for working with large volume spatial data. Quick start tutorials. *Geosoft Incorporated, Toronto*, 258 pp.
- Grenne, T. (1989) Magmatic evolution of the Løkken SSZ Ophiolite, Norwegian Caledonides: relationships between anomalous lavas and high-level intrusions. *Geological Journal*, **24**, 251-274.
- Grenne, T., Grammelvedt, G. and Vokes, F.M. (1980) Cyprus-type sulphide deposits in the western Trondheim district, central Norwegian Caledonides. In Panayiotou, A. (ed.) *Ophiolites*. Proceedings of the International Ophiolite Symposium, Cyprus, 1979. *Geological Survey of Cyprus, Nicosia*, pp. 727-743.
- Håbrekke, H. (1983) Geofysiske målinger fra helikopter over et område nord for svenskegrensen i Lierne og Snåsa kommuner, Nord-Trøndelag fylke. *Norges geologiske undersøkelse Rapport 1898*, 12 pp + 8 maps.
- Kero, L. and Johansson, R. (2006) Raudfjellet; modellberäkning. *Sveriges Geologiska Undersökning Rapport 08-733/2006*, 12 pp.
- Mogaard, J.O. (2006) Data Acquisition and Processing – Helicopter Geophysical Survey, Skjaekerdalen, 2006 Nord-Troendelag county, Norway. *Norges geologiske undersøkelse Report 2006.041*, 11 pp.
- Nilsson, L.P. (2000) Oppfølgingsarbeider på magnesitt, talk og kleberstein i Raudfjellet, Snåsa. *Norges geologiske undersøkelse Rapport 2000.57*, 133 pp + 1 map at 1:10 000 scale.

- Nilsson, L.P., Sturt, B.A. and Ramsay, D.M. (1999) Ophiolittundersøkelser i Snåsa og Lierne: en rekognosering for å påvise mulig interessante forekomster av malm, industrimineraler og naturstein. *Norges geologiske undersøkelse Rapport* 1999.114, 92 pp + 1 map at scale 1:10 000.
- Nilsson, L.P., Roberts, D. and Ramsay, D.M. (2005) The Raudfjellet ophiolite fragment, Central Norwegian Caledonides: principal lithological and structural features. *Norges geologiske undersøkelse Bulletin*, **445**, 101-117.
- Nilsson, L.P. and Roberts, D. (2014) A trail of ophiolitic debris and its detritus along the Trøndelag-Jämtland border: correlations and palaeogeographical implications. *Norges geologiske undersøkelse Bulletin*, **453**, 29 - 41.
- Roberts, D. (1997a) Geologisk kart over Norge. Berggrunnsgeologisk kart GRONG, M 1:250 000. *Norges geologiske undersøkelse*.
- Roberts, D. (1997b) Geochemistry of Palaeoproterozoic porphyritic felsic volcanites from the Olden and Tømmerås windows, Central Norway. *Geologiska Föreningens i Stockholm Förhandlingar*, **119**, 141-148.
- Roberts, D. and Gee, D.G. (1985) An introduction to the structure of the Scandinavian Caledonides. In Gee, D.G. and Sturt, B.A. (eds.) *The Caledonide Orogen – Scandinavia and related areas*. John Wiley & Sons, Chichester, pp. 55-68.
- Roberts, D., Nissen, A.L. and Walker, N. (1999) U-Pb zircon age and geochemistry of the Blåfjellhatten granite, Grong-Olden Culmination, Central Norway. *Norsk Geologisk Tidsskrift*, **79**, 161-168.
- Roberts, D., Walker, N., Slagstad, T., Solli, A. and Krill, A. (2002) U-Pb zircon ages from the Bymarka ophiolite, near Trondheim, Central Norwegian Caledonides, and regional implications. *Norsk Geologisk Tidsskrift*, **82**, 19-30.
- Schrotter, J.-M., Pagé, P., Bédard, J.H., Tremblay, A. and Bécu, V. (2003) Forearc extension and sea-floor spreading in the Thetford Mines Ophiolite Complex. In: Dilek, Y. & Robinson, P.T. (eds) *Ophiolites in Earth History*. Geological Society, London, Special Publications, 218, 231-251.
- Sjöström, H. and Bergman, S. (1989) Asymmetric extension and Devonian(?) normal faulting: examples from the Caledonides of eastern Trøndelag and western Jämtland. (Extended abstract) *Geologiska Föreningens i Stockholm Förhandlingar*, **111**, 407-410.
- Sjöström, H. and Roberts, D. (1992) Gjevsjøen, berggrunnskart 1823-2, 1:50 000, foreløpig utgave. *Norges geologiske undersøkelse*.
- Sjöström, H. and Roberts, D. (2013) Gjevsjøen, berggrunnskart 1823-2, 1:50 000, revidert foreløpig utgave; digitalt fargeplott. *Norges geologiske undersøkelse*.
- Slagstad, T. (2003) Geochemistry of trondhjemites and mafic rocks in the Bymarka ophiolite, Trondheim, Norway: petrogenesis and tectonic implications. *Norwegian Journal of Geology*, **83**, 167-185.
- Törnebohm, A.E. (1896) Grunddragen af det centrala Skandinaviens bergbyggnad. *Kongliga Svenska Vetenskaps-Akademiens Handlingar*, **28** (5), 212 pp.
- Troëng, B. (1982) Uranium-rich granites in the Olden window, Sweden. *Mineralogical Magazine*, **46**, 217-226.